



HAL
open science

**Expanding the phenotype of mitochondrial disease:
Novel pathogenic variant in ISCA1 leading to instability
of the iron-sulfur cluster in the protein**

E Lebigot, M Hully, L Amazit, P Gaignard, T Michel, M Rio, Marc Lombès,
P Thérond, A Boutron, Marie-Pierre Golinelli

► **To cite this version:**

E Lebigot, M Hully, L Amazit, P Gaignard, T Michel, et al.. Expanding the phenotype of mitochondrial disease: Novel pathogenic variant in ISCA1 leading to instability of the iron-sulfur cluster in the protein. *Mitochondrion*, 2020, 10.1016/j.mito.2020.02.008 . hal-02971951

HAL Id: hal-02971951

<https://hal.science/hal-02971951>

Submitted on 19 Oct 2020

HAL is a multi-disciplinary open access archive for the deposit and dissemination of scientific research documents, whether they are published or not. The documents may come from teaching and research institutions in France or abroad, or from public or private research centers.

L'archive ouverte pluridisciplinaire **HAL**, est destinée au dépôt et à la diffusion de documents scientifiques de niveau recherche, publiés ou non, émanant des établissements d'enseignement et de recherche français ou étrangers, des laboratoires publics ou privés.



Expanding the phenotype of mitochondrial disease: Novel pathogenic variant in *ISCA1* leading to instability of the iron-sulfur cluster in the protein

E. Lebigot^{a,b,*}, M. Hully^c, L. Amazit^{d,e}, P. Gaignard^a, T. Michel^b, M. Rio^f, M. Lombès^d, P. Thérond^a, A. Boutron^a, M.P. Golinelli-Cohen^b

^a Biochemistry Department, Hôpital Bicêtre, APHP Université Paris-Saclay, Le Kremlin Bicêtre F-94275, France

^b Université Paris-Saclay, CNRS, Institut de Chimie des Substances Naturelles, UPR 2301, 91198 Gif-sur-Yvette, France

^c Pediatric Neurology Department, Hôpital Necker Enfants Malades, Institut Imagine, APHP Centre – Université de Paris, Paris F-75015, France

^d Institut National de la Santé et de la Recherche Médicale Unité 1185, Unité Mixte de Recherche Faculté de Médecine Paris-Sud, Université Paris-Sud, Université Paris Saclay, Le Kremlin Bicêtre F-94276, France

^e Unité mixte de Service 32, Institut Biomédical de Bicêtre, Le Kremlin-Bicêtre F-94276, France

^f Genetic Department, Hôpital Necker Enfants Malades, Institut Imagine, APHP Centre – Université de Paris, Paris F-75015, France

ARTICLE INFO

Keywords:

MMDS
ISCA1
Iron-sulfur cluster
PDH
Lipoic acid

ABSTRACT

We report a patient carrying a novel pathogenic variant p.(Tyr101Cys) in *ISCA1* leading to MMDS type 5. He initially presented a psychomotor regression with loss of gait and language skills and a tetrapyramidal spastic syndrome. Biochemical analysis of patient fibroblasts revealed impaired lipoic acid synthesis and decreased activities of complex I and II of respiratory chain. While *ISCA1* is involved in the mitochondrial machinery for iron-sulfur cluster biogenesis, these dysfunctions are secondary to impaired maturation of mitochondrial proteins containing the [4Fe-4S] clusters. Expression and purification of the human *ISCA1* showed a decreased stability of the [2Fe-2S] cluster in the mutated protein.

1. Introduction

In mammals, the mitochondrial machinery for iron-sulfur cluster (ISC) biogenesis requires at least 18 proteins (Braymer and Lill, 2017). Three major steps are necessary for the formation of the ISC and its delivery to recipient proteins. The first step is the *de novo* assembly of a [2Fe-2S] cluster on the scaffold protein ISCU using inorganic iron and sulfur ions. Then, the cluster is transferred to a first temporary recipient protein (GLRX5) and secondarily to mitochondrial Fe-S-assembling proteins (Beilschmidt and Puccio, 2014). Maturation of [2Fe-2S]-containing proteins can directly proceed from GLRX5, while maturation of the [4Fe-4S]-containing proteins requires supplementary steps with the biosynthesis of [4Fe-4S] cluster and its delivery to mitochondrial [4Fe-4S] proteins. Five proteins, *ISCA1*, *ISCA2*, *BOLA3*, *NFU1* and *IBA57*, are involved in these last steps but the precise role of each of these proteins is not yet completely understood. Several *in vitro* studies suggested that *ISCA1* and *ISCA2* are essential for the biosynthesis of [4Fe-4S] clusters from [2Fe-2S]-containing GLRX5 (Brancaccio et al., 2014; Brancaccio et al., 2017). *NFU1* and

BOLA3 seem to be dedicated to [4Fe-4S] cluster delivery to client apoproteins including *LIAS* and *SDHB* (Cameron et al., 2011; Melber et al., 2016). *IBA57* could also take part in [4Fe-4S] cluster biogenesis or [4Fe-4S] cluster transfer to recipient apoproteins (Sheftel et al., 2012; Ajit Bolar et al., 2013; Gourdoups et al., 2018). Mutations in genes encoding for *NFU1*, *BOLA3*, *IBA57*, *ISCA2* and *ISCA1* lead to multiple mitochondrial dysfunction syndrome (MMDS) types 1 to 5, respectively. In 2017, the first four patients from two Indian families with MMDS type 5 were described and associated to the homozygous p.(Glu87Lys) pathogenic variant in *ISCA1* (Shukla et al., 2017). Then, a similar fifth case was reported (Shukla et al., 2018). Finally, an Italian patient carrying a novel homozygous pathogenic variant p.(Val10Gly) in *ISCA1* was described with extended biochemical investigation (Torraco et al., 2018).

Herein, we report a young boy from Egyptian origin carrying a novel pathogenic variant in *ISCA1* leading to the yet undescribed p.(Tyr101Cys) mutation in *ISCA1*. A tetrapyramidal spasticity episode and skills regression were noted at 20 months of age associated with cavitating leukodystrophy on brain imaging. At 4 years of age, he

Abbreviations: BN-PAGE, Blue-native polyacrylamide gel electrophoresis; CSF, Cerebro-spinal fluid; ISC, Iron-sulfur cluster; α -KGDHC, Alpha-ketoglutarate dehydrogenase; MMDS, Multiple mitochondrial dysfunction syndrome; NGS, Next-generation sequencing; OCR, Oxygen consumption rate; PBS, Phosphate-buffered saline; PDHC, Pyruvate dehydrogenase complex; RC, Respiratory chain; WT, Wild-type

* Corresponding author at: Biochemistry Department, Hôpital Bicêtre, APHP Université Paris-Saclay, Le Kremlin Bicêtre F-94275, France.

E-mail address: elise.lebigot@aphp.fr (E. Lebigot).

<https://doi.org/10.1016/j.mito.2020.02.008>

Received 8 November 2019; Received in revised form 31 January 2020; Accepted 19 February 2020

Available online 21 February 2020

1567-7249/© 2020 Elsevier B.V. and Mitochondria Research Society. All rights reserved.

recovered walking with easy fatigability but language was severely delayed. Investigation in fibroblasts from the patient showed that lipoic acid synthesis was impaired and activities of complex I and II of respiratory chain were also decreased. Thus, ISCA1 deficiency leads to dysfunction of mitochondrial [4Fe-4S]-containing proteins either involved in lipoic acid synthesis (LIAS) or essential for complexes I and II activities. After bacterial overexpression, purification of human ISCA1 showed that the p.(Tyr101Cys) mutation leads to an increased instability of its Fe-S cluster. This report shows similarities with well documented other MMD5 types 1 to 4 but reveals that clinical feature of MMD5 type 5 is wide ranging from early onset and fatal encephalopathy to more moderate symptomatology with predominant spasticity and neurodevelopmental delay. Thereafter, patients with pathogenic variant in *ISCA1*, *ISCA2* or *IBA57* will be respectively named *ISCA1*, *ISCA2* or *IBA57* patients to facilitate the reading of the manuscript.

2. Materials and methods

2.1. Cell culture

Individuals without mitochondrial disease were referred as control subjects. Cultured skin fibroblasts were grown in Ham's F-10 medium (Eurobio, Les Ulis, France) supplemented with antibiotics (100 IU/mL penicillin and 100 µg/mL streptomycin), 50 mg/L uridine and 12% fetal bovine serum (Life Technologies, Carlsbad, CA, USA) for fibroblasts and 20% fetal bovine serum for myoblasts. Cells were cultured at 37 °C in a humidified incubator with 5% CO₂. Cultured myoblasts from the *ISCA1* patient were obtained from Biobank of Cochin Hospital (Paris). Clinical, biochemical and brain imaging data were collected retrospectively. Informed consent prior to skin biopsy was obtained from parents of patients included in this study.

2.2. Biochemical studies

PDHc activity in fibroblasts was carried out as described (Imbard et al., 2011). Polarographic or spectrophotometric assays of mitochondrial respiratory chain (RC) complexes, α -KGDHc and citrate synthase activities were measured according to standard procedures (Rustin et al., 1994). Complex I activity assay was performed on mitochondrial enriched fractions prepared from permeabilized cells with digitonin as previously described (Chretien et al., 2003). RC complex activity was normalized to citrate synthase activity.

2.3. Immunoblot and BN-PAGE analysis

Western blot analysis was performed on mitochondria-enriched fractions or on total cell lysates. About 30 µg of protein extracts were separated by SDS-PAGE and transferred to PVDF membranes, blocked in PBS-Tween containing 5% non-fat milk and then incubated overnight with primary antibodies. Following antibodies directed against lipoic acid (LA) (Abcam, ab58724), ISCA1 (ThermoFisher, PA5-60121), SDHB (Abcam, ab14714), Rieske protein (Abcam, ab14746), ferrochelatase (kindly provided by Dr. H. Puccio, Strasbourg, France), mt-aconitase (kindly provided by Dr. R. B. Franklin, University of Maryland, Baltimore, USA), GRIM19 (Abcam, ab10240), GAPDH (Sigma-Aldrich, G9545) and prohibitin (Novusbio, NBP2-37563) were used. Secondary peroxidase-conjugated anti-mouse (Sigma-Aldrich, A4416) and anti-rabbit (Sigma-Aldrich, NA934V) antibodies were used. Detection was achieved using the ECL chemiluminescence kit (GE Healthcare) and G-Box (Syngene) associated with GeneSNAP software. Blue-native PAGE (BN-PAGE) analysis was carried out on mitochondria-enriched fractions from fibroblasts (Hescot et al., 2013). Immunoblotting was performed using antibodies raised against the complex I subunit GRIM19 (Abcam, ab10240), the 70 kDa subunit of complex II (SDHA, Abcam, ab14715), the complex III subunit core2 (UQCRC2, Abcam, ab14745) and the MTCO1 subunit of complex IV (Abcam, ab110270).

2.4. Molecular analysis

Genomic DNA was extracted from fibroblasts by standard methods on automated nucleic acid extraction system QIASymphony (Qiagen) and molecular analysis was performed using next-generation sequencing (NGS). The entire coding exons (\pm 50 bp) of a panel of 117 genes related to mitochondrial diseases, including pyruvate crossing abnormalities and mitochondrial cytopathies were analyzed. This panel was designed using the Agilent Sure Design web application (Agilent). Preparation of genomic DNA for NGS analysis and bioinformatics workflow were performed as previously described (Bouali et al., 2017). High Throughput Sequencing was performed on an Illumina MiSeq instrument. Sanger sequencing was performed after PCR amplification with specific primers to validate the identified *ISCA1* mutation and to analyze parental DNAs. The integrated software ALAMUT V.2.7 (Interactive Biosoftware; <http://www.interactive-biosoftware.com> including Align GVGD, SIFT and MutationTaster) and Polyphen2 software were used for *in silico* analysis of DNA variant.

2.5. Mitochondrial network study

Skin fibroblasts were seeded at subconfluence on a glass coverslip and incubated for 40 min in darkness at 37 °C with 0.1 µM MitoTracker Red CMXRos (Invitrogen, M7512) in Ham's F-10 medium. Cells were rinsed with PBS and then fixed in 4% paraformaldehyde in PBS. Lastly, cells were incubated for 1 min with 1 µg/mL Hoechst (Invitrogen, H3570) in PBS. Fluorescent cells were observed with an Olympus Provis AX70 (Rungis, France), and images were acquired with Qcapture Pro version 5.1 (Q Imaging Inc., Surrey, British Columbia, Canada) using an Evolution VF Monochrome camera (Media Cybernetics Inc., Bethesda, MD).

2.6. Expression and purification of mature ISCA1

The mature form of human ISCA1 (NCBI Q9BUE6, residues 24–129) and the p.Tyr101Cys mutated form were expressed in *E. coli* using the pET28a vector (GenScript). The N-term His-tagged proteins were expressed using Rosetta(DE3)pLys cells in an 2xTY medium with 50 mg/L kanamycin at 37 °C. At OD₆₀₀ = 0.5, 25 µM FeCl₃ was added and the temperature was decreased to 18 °C. Forty minutes later, 0.2 mM IPTG was added to the medium. Cells were cultured at 18 °C for 20 h and then harvested by centrifugation for purification steps. Bacterial pellets were re-suspended in 50 mL of Lysis Buffer (50 mM Tris-HCl pH 8, 500 mM NaCl, 5 mM imidazole, 0.1% triton X100, 1 mM DTT) containing an antiprotease cocktail (P2714; Sigma-Aldrich). After sonication and ultracentrifugation (1h at 70,000xg), the cleared lysate was applied to a 5 mL HiTrap chelating HP column (GE Healthcare) on an Äkta FPLC (GE Healthcare) pre-equilibrated with Lysis Buffer. Proteins were eluted using a 0–60% linear gradient between Lysis buffer and Elution Buffer (50 mM Tris-HCl pH 8, 500 mM NaCl, 500 mM imidazole). Fractions containing ISCA1 were pooled and concentrated using an Amicon Ultra-15 centrifugal filter unit (Millipore) with a 5 kDa cutoff. Protein purity was assessed to be > 99% using SDS-PAGE. Protein concentrations were measured using Bradford assay with bovine serum albumin as standard (Bradford, 1976). Protein aliquots were frozen in liquid nitrogen. UV-visible absorption spectra were recorded between 240 and 900 nm with a Cary 100 (Agilent) spectrophotometer.

2.7. Iron quantification

Iron content in purified protein was quantified using a bathophenanthroline colorimetric assay adapted from (Fish, 1988). For total iron quantification of a 38.6 µL protein sample, 2.9 µL of perchloric acid 54% was added. After 30 min at room temperature, 20.6 µL of bathophenanthroline sulfonate 1.7 mg/mL, 5.1 µL of sodium ascorbate 76 mg/mL and 2.9 µL of saturated ammonium acetate solution were added and the reaction was completed with water up to 100 µL. After

30 min at room temperature, the absorbance at 535 nm was measured. Mohr's salt solution was used as standard.

3. Results

3.1. Case report

The boy, sixth child from consanguineous parents native from Egypt, was born at 31 weeks of pregnancy by caesarean delivery due to retro-placental hematoma. He was able to walk at 18 months of age and to pronounce some syllables at about 20 months. At this age, an episode of motor deficiency of the left arm occurred. Neurological examination showed tetrapyramidal syndrome with spasticity of the limbs, and no neuropathy. After this episode, regression of skills was noted with loss of independent walking and language. At 30 months of age, he partially recovered and was able to walk few steps with help. The left arm also partially recovered but remained weak. At 4 years and a half, he presented with spastic diplegia enabling him walking despite frequent falls and fatigability. He was then able to say isolated few words. The brain MRI (bMRI) performed at 20 months of age showed leukodystrophy without calcifications on cerebral scan. At 2 years old, electro-neuromyogram showed no peripheral neuropathy. BMRI revealed cavitating leukodystrophy with diffuse lesions of periventricular supratentorial white matter with hyperintensity on T2 ponderation images and with hypointensity on T1 ponderation sequences, sparing U fibers. Apparent diffusion coefficient was decreased. Vacuolization was found in supratentorial white matter, not in the corpus callosum. A mild ventriculomegaly and a thin corpus callosum were observed. No cortical malformation was detected. At 4 years of age, bMRI remained otherwise stable (Fig. 1, panels A, B, C and D) and brain spectroscopy detected a lactate peak (Fig. 1, panel E). Lactate was high in blood (3.2 mmol/L; reference values (RV): < 2.0 mmol/L) with elevated pyruvate (0.23 mmol/L; RV: < 0.15 mmol/L) but lactate/pyruvate ratio was in the normal range (13.9; RV: 12.0–18.0). All other biological investigations were unremarkable including extensive metabolic screening for lysosomal and peroxysomal diseases as well as for interferonopathies. Pyruvate dehydrogenase (PDH) deficiency and mitochondrial cytopathy were also suspected to cause the clinical feature of this patient.

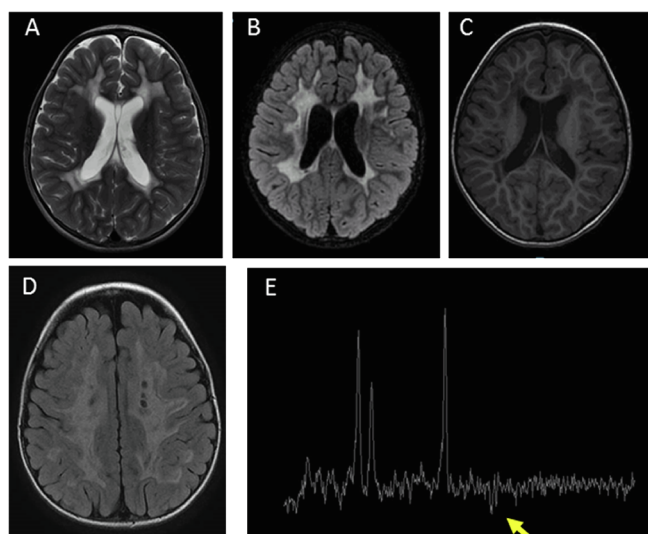


Fig. 1. Images of brain MRI and brain spectroscopy of the *ISCA1* patient. Cavitating leukodystrophy with diffuse lesions of periventricular supratentorial white matter with hyperintensity on T2 (A) and flair (B) and with hypointensity on T1 (C). (D) Vacuolization was located in supratentorial white matter. (E) Lactate peak on brain spectroscopy is pointed out by a yellow arrow.

Table 1

Oxygen consumption rate (OCR), α -KGDHc-, PDHc- and respiratory chain complex activity assays performed on primary cultured skin fibroblasts of the *ISCA1* patient.

	Result	Reference values
<i>O₂ consumption rate in permeabilized cells (nmol O₂/min/mg of protein)</i>		
Oxidation of pyruvate	2.8	2.6–4.9
Oxidation of succinate	4.6	5.2–9
Oxidation of glycerol-3-phosphate	3.8	3.4–5.5
Oxidation of decylubiquinol	9.4	6.6–10.6
<i>Activity of tricarboxylic acid cycle enzymes (nmol/min/mg of protein) and PDH complex (pmol/min/mg of protein)</i>		
Citrate synthase	47	31–65
α -KGDHc	3.7	3.6–7.2
PDHc	1013	1170–3104
<i>Activity of respiratory chain complexes (nmol/min/mg of protein)</i>		
Complex II	11	11–19
Complex III	69	33–67
Complexes II + III	20	14–29
Complex IV	64	41–81
<i>Relative enzymatic activities of respiratory chain complexes</i>		
Complex IV/Complex II ratio	5.82	2.70–5.30
Complex II/citrate synthase	0.23	0.24–0.38
Complex IV/citrate synthase	1.36	0.90–1.60

Citrate synthase activity served as mitochondrial content control. Values in bold indicate results outside of the normal value range.

3.2. Biochemical analyses

Oxygen consumption rate (OCR), PDH activity and respiratory chain complexes activity assays were performed in primary cultured skin fibroblasts of the patient when he was 30 months old. Results are presented in Table 1.

These results showed a moderate decrease of PDHc activity and a marked decreased OCR with succinate, suggesting dysfunction of complex II. It was confirmed by a slightly decreased activity of complex II and decreased complex II/citrate synthase activities ratio without any observable effect of the other RC complex activities compared to reference values. These observations led us to analyze DNA of the patient by NGS analysis on our panel of nuclear genes dedicated to mitochondrial diseases.

3.3. Molecular results

Applying filters for variations with low allelic frequency (< 0.03 in 1000 genome DATABASE), the analysis of NGS data sets revealed a homozygous variation (c.302A > G; p.Tyr101Cys) located in exon 4 of *ISCA1* (NM_030940.4) (Fig. 2, part A). Seventy other variants were identified including 3 variants predicted as deleterious in genes *ACAD9*, *SDHD* and *COQ6* at the heterozygous state. Mutations in these genes are related to mitochondrial disease with recessive transmission and no other gene variation (intragenic deletion or insertion) was detected in these three genes. Thus, the homozygous *ISCA1* mutation remained the only candidate for the observed phenotype and the biochemical data. We validated this variant by family analysis showing that each parent of the patient carried the *ISCA1* mutation at the heterozygous state. This *ISCA1* variation was never reported before (in 1000 genome, dbSNP and EXAC databases) and was predicted as a deleterious variant by *in silico* analysis using prediction softwares

3.4. Biochemical consequences of the Tyr101Cys mutation in *ISCA1*

3.4.1. Characterization of the purified protein

First, we overexpressed the native form of human *ISCA1* (deletion of the mitochondrial targeting signal formed by the first 23 residues) in *E. coli* fused to an N-terminal His-tag. Even if Fe-S proteins are known to

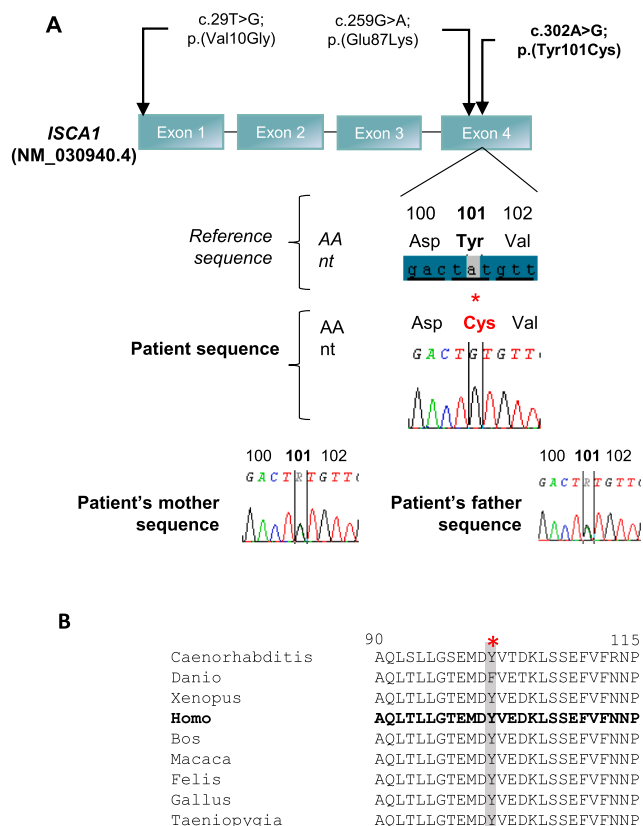


Fig. 2. Localization of the novel variant in *ISCA1* and conservation of residue 101 in *ISCA1* protein in different orthologues. (A) Sanger validation of the variant in exon 4 of *ISCA1* in the patient and his parents. Other variants reported in *ISCA1* are localized in exon 4 (10) and in exon 1 (12). (B) Alignment of *ISCA1* protein from different species with CLUSTAL O(1.2.4) multiple sequence alignment from NCBI orthologues sequences. Residue Tyr (Y) number 101 in Homo sapiens, noted with red star, is conserved in all represented species except Danio i.e. zebrafish.

be sensitive to oxygen, previous anaerobic purification of mouse *ISCA1* leads to protein precipitation (Beilschmidt et al., 2017). Then, we purified the overexpressed protein under aerobic conditions and obtained a colored WT protein. The UV-visible spectra of the as-purified *ISCA1* is characterized by absorption bands at 320 and 420 nm and shoulders at 460 and 550 nm (Fig. 3, panel A). These results are compatible with the presence of a [2Fe-2S] cluster in the aerobically purified WT form of *ISCA1*. Then, we expressed the Tyr101Cys mutated form of human *ISCA1* and purified it using similar conditions than those used for the WT form. We obtained a colorless protein. The absence of cluster was confirmed by the UV-visible absorption spectrum, which does not present any significant absorption in the visible part (Fig. 3, panel A). Chemical analysis confirmed that the as-purified Tyr101Cys mutated form contains only low amounts of iron compared to the WT form (Fig. 3, panel B). Thus, aerobic purifications of overexpressed mature *ISCA1* led to a [2Fe-2S] cluster-containing WT form while Tyr101Cys form lacks its Fe-S cluster.

3.4.2. Western blot

To further confirm and better understand the molecular consequences of the *ISCA1* Tyr101Cys mutation, we extended the biochemical investigation. We first looked at *ISCA1* protein level in the patient fibroblasts compared to fibroblasts of patients with either deficiency in *ISCA2* or in *IBA57* (P12 and P10 respectively, described in our previously published study (Lebigot et al., 2017)). Immunoblot analysis revealed a statistical lower amount of *ISCA1* protein in *ISCA1* patient fibroblasts compared to the control fibroblasts (Fig. 4B). *ISCA1*

protein amount in *ISCA2* or *IBA57* patient was similar to those of controls.

In addition, we performed some analysis to evaluate how *ISCA1* deficiency could affect maturation of ISC protein in the patient fibroblasts. We first looked at the level of lipoylation of the E2 subunit of PDHc and of α -KGDHc to evaluate the enzymatic activity of LIAS which is dependent on the insertion of its [4Fe-4S] cluster (Landgraf et al., 2016) (Fig. 5A). Furthermore, we examined the levels of several mitochondrial [2Fe-2S]- and [4Fe-4S]-containing proteins (Fig. 5B and C). Finally, several other subunits of RC complexes were tested. We found an alteration of the lipoylation of PDH-E2 and a more severe decrease for α -KGDH-E2, likely secondary to a LIAS dysfunction. We also observed a marked decrease in SDHB expression in the patient fibroblasts. Other proteins of complex II and of complex I, which do not contain ISC (SDHA and GRIM19, respectively), and proteins carrying a [2Fe-2S] cluster (Rieske protein of complex III and ferredoxin) were not affected by the *ISCA1* deficiency.

3.4.3. RC and TCA functionality in fibroblasts and myoblasts

We further studied the consequences of *ISCA1* deficiency on RC complexes and TCA enzymes activities in fibroblasts. As shown in Table 1, RC complexes and α -KGDHc activities were only weakly affected by *ISCA1* deficiency, despite lipoylation defect (Fig. 5A) and decreased level of SDHB protein (Fig. 5C). We explored these enzymatic activities in myoblasts to evaluate if this cellular type would be more affected than fibroblasts (Fig. 6). Complex I activity was decreased in fibroblasts but unfortunately, limitation in the amount of cellular material did not allow us to measure complex I activity in myoblasts. Both results in myoblasts and in fibroblasts showed decreased complex II activity while others enzymatic activities were near values obtained in control cells.

BN-PAGE analysis was performed using fibroblasts to assess the RC complex assembly (Fig. 7). This experiment underlined the effects on the integrity of complexes I and II and revealed additional effects on complex IV.

Our investigations showed several mitochondrial damages in *ISCA1* deficient fibroblasts including RC complexes and lipoic acid metabolism dysfunction. As mitochondrial network morphology can vary from hyperfused to fragmented morphology in accordance with OXPHOS activities or nutrient status (Wai and Langer, 2016), we questioned whether mitochondrial network morphology could be affected in fibroblasts of patient with *ISCA1* deficiency. We observed *ISCA1* patient cells after incubation with MitoTracker Red CMXRos® which stains functional mitochondria and found similar tubular mitochondrial network with homogenous cellular distribution in patient and in control fibroblasts (Fig. 8).

4. Discussion

Pathogenic variants in genes encoding for proteins involved in the late step of the mitochondrial ISC machinery lead to various types of MMDS pathology. MMDS type 5, caused by mutations in *ISCA1*, was recently described in 5 patients from three Indian families (Shukla et al., 2017; Shukla et al., 2018) and one Italian patient (Torraco et al., 2018). MMDS type 5 leads to early-onset, fatal encephalopathy and/or severe spasticity and seizures (Shukla et al., 2017; Shukla et al., 2018; Torraco et al., 2018) and resembles MMDS types 3 and 4 due to pathogenic variants in *IBA57* and *ISCA2*, respectively (Ajit Bolar et al., 2013; Lebigot et al., 2017; Lossos et al., 2015; Debray et al., 2015; Al-Hassnan et al., 2015). Extensive leukodystrophy on brain MRI and ophthalmic symptoms such as optic atrophy or nystagmus were described in most of the patients with MMDS type 3, 4 or 5. The present article describes a new patient with *ISCA1* deficiency. This patient from Egyptian origin presented with a psychomotor regression with transient loss of gait at 20 months of age. He progressively recovered but, at 4 years of age, he remained impaired with spastic diplegia leading to recurrent falls while walking associated with

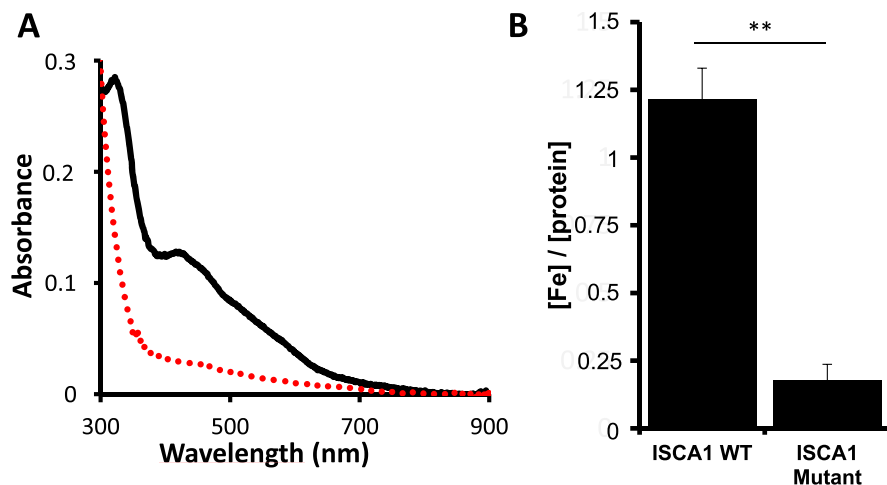


Fig. 3. UV-visible absorption spectra and iron content analysis of purified WT and Tyr101Cys mutant. (A) UV-visible spectra of the WT (black line) and Tyr101Cys (red dotted line) forms of purified ISCA1 at 40 μ M. (B) Iron contents of purified ISCA1 forms. Results were expressed as the ratio of the iron and the protein concentrations. Data represent mean \pm SEM of 3 independent experiments. Statistical analysis: *t*-test (significance: ***p* < 0.01).

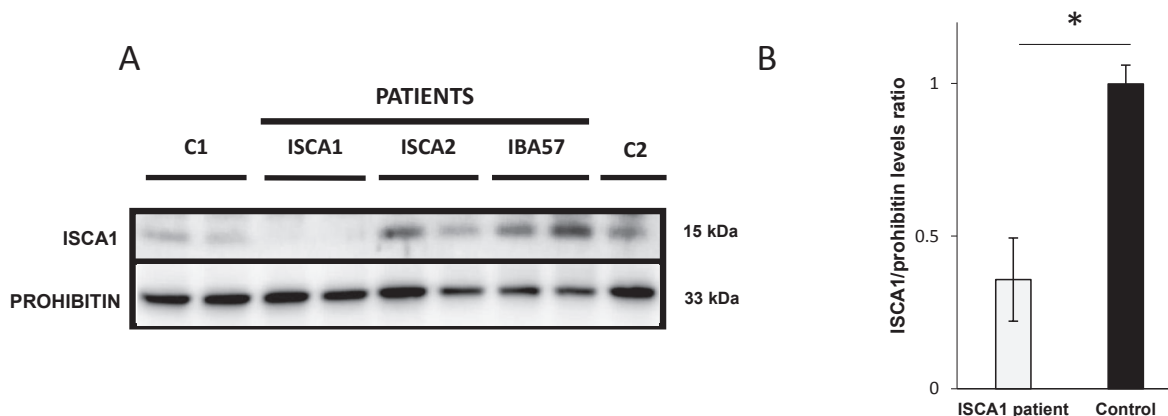


Fig. 4. ISCA1 protein levels in fibroblasts of patients carrying *ISCA1*, *ISCA2* or *IBA57* pathogenic variants. (A) Mitochondrial enrichments of fibroblasts (from patients and controls C1 and C2) were analyzed using ISCA1 antibody. Samples were loaded twice. Prohibitin is shown as the loading control of mitochondrial content. (B) Data present ISCA1 protein level over prohibitin protein level in ISCA1 patient fibroblasts and in control fibroblasts. Data represent mean \pm SEM of 4 independent experiments. Statistical analysis: paired Student test. Significance: **p* < 0.05.

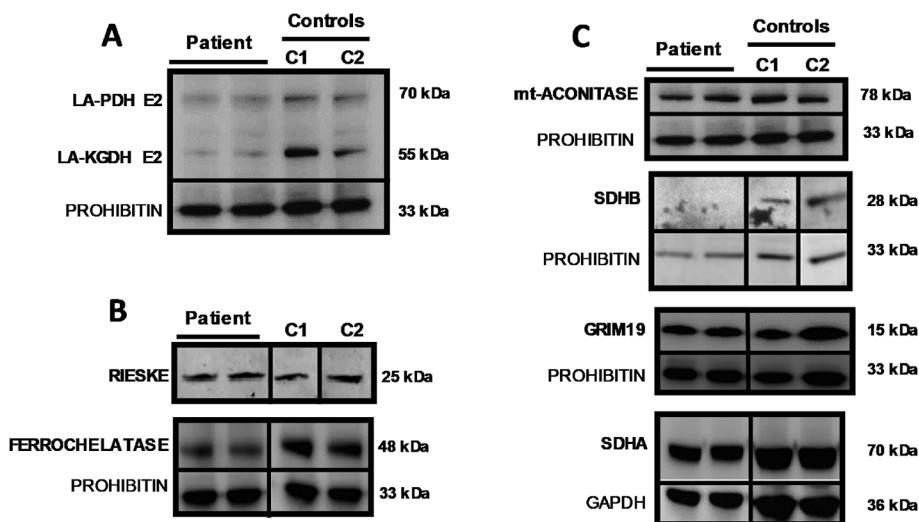


Fig. 5. Protein levels of mitochondrial Fe-S proteins in fibroblasts of patient with *ISCA1* pathogenic variant. (A) Lipoylated proteins were detected using antibody against lipoic acid. (B) Levels of mitochondrial [2Fe-2S] proteins (Rieske and ferrochelatase). (C) Levels of [4Fe-4S]-containing proteins (mt-aconitase and SDHB) and proteins involved in complex I (GRIM19) or complex II (SDHA). Samples of patient were loaded twice. Prohibitin serves as loading control for samples obtained after mitochondrial enrichment and GAPDH serves as loading control for total cell lysate samples. For each antibody, all the samples were analyzed on the same gel; however, unnecessary lanes were removed and replaced by black lines.

fatigability and severe language deficiency. Thus, his clinical symptoms, despite less severe, were similar to the Italian patient ones. As for this latter and others patients with MMDS (de Souza et al., 2018), bMRI of the French patient revealed abnormalities. Cavitating leukodystrophy, ventriculomegaly and thin corpus callosum were observed similar to the described patients with MMDS type 5 especially the Italian one, but with

less impairment. All the previously reported *ISCA1* patients died between 11 months and 11 years of age. Currently, the patient that we described here is 6 years old and keep improving skills. MMDS 3 and 4 also led to variable clinical symptomatology and evolution. Thus, *IBA57* or *ISCA2* patients display variable clinical features closed to those observed in *ISCA1* patients with progressive neurological regression and

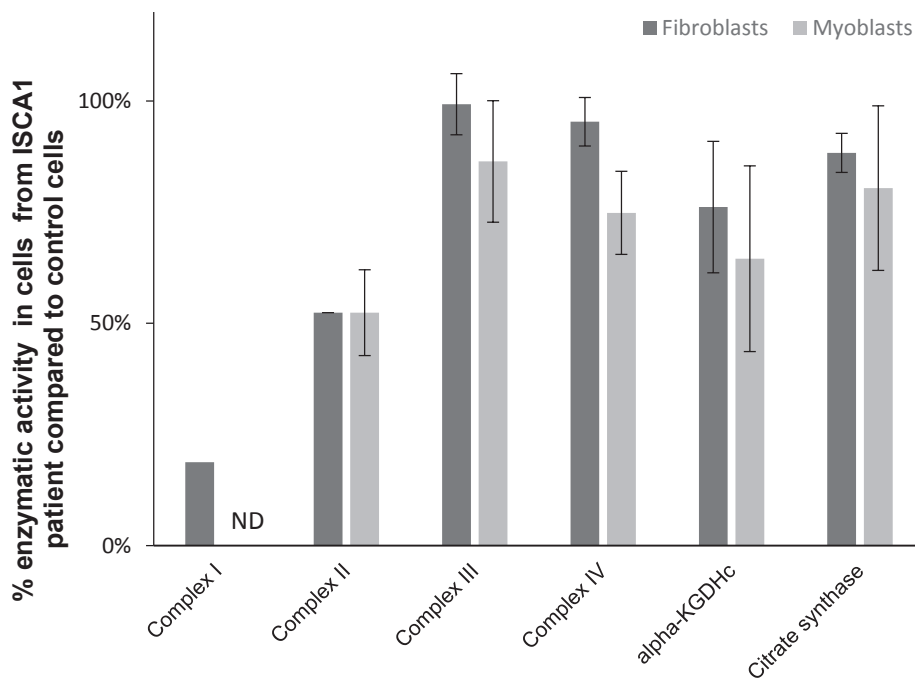


Fig. 6. Activities of RC complexes and TCA enzymes (citrate synthase and alpha-KGDHc) in fibroblasts and myoblasts of the *ISCA1* patient. Activities were compared to those of control cells (fibroblasts and myoblasts respectively) measured in same conditions, in total cell lysates or in mitochondrial enriched fractions (complex I only). Citrate synthase activity was used as an indication for mitochondrial content. Data represent mean \pm SEM of 2 independent experiments except for complex I activity (only one experiment in fibroblasts and no analysis in myoblasts; ND: not done)

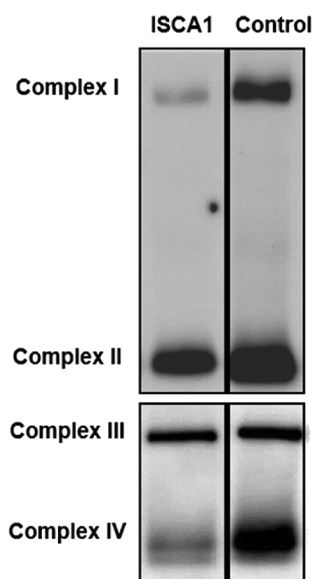


Fig. 7. Blue-native PAGE analysis of respiratory chain complexes. BN-PAGE analysis of mitochondrial enriched fibroblasts of the *ISCA1* patient and control was performed using antibodies against respiratory chain complex subunits without [Fe-S] cluster (complex I: GRIM19, complex II: SDHA, complex III: UQCRC2, complex IV: MTCO1). Results for both samples are issued from the same experiment that needed two different gels represented in two blocks (unnecessary lanes were removed and replaced by black lines).

leukodystrophy or severe encephalopathy with early onset and sometimes early death (Ajit Bolar et al., 2013; Lossos et al., 2015; Toldo et al., 2018; Debray et al., 2015; Al-Hassnan et al., 2015; Ishiyama et al., 2017; Torraco et al., 2017; Hamanaka et al., 2018; Liu et al., 2018; Alfadhel et al., 2018; Alaimo et al., 2018). Among all reported patients, no optic atrophy was reported for *ISCA1* patients while it was frequent in *IBA57* or *ISCA2* patients (Al-Hassnan et al., 2015; Hamanaka et al., 2018). Only nystagmus and visual impairment were present in the Italian *ISCA1* patient (Torraco et al., 2018).

The novel *ISCA1* homozygous variant (p.(Tyr101Cys)), the third to be described, that we identified, led to a reduction in the level of *ISCA1*

protein in fibroblasts. This observation suggests that mutated protein could be degraded due to abnormal protein folding even though we did not explore this hypothesis further. Overexpression and purification of WT *ISCA1* and of the mutated form confirmed that mutation of Tyr101, a residue close to the Fe-S cluster, leads to cluster destabilization. Two other mutations were described previously. The p.(Val10Gly) mutation, involving a residue from the mitochondrial targeting peptide, led to decrease of the mitochondrial import of the protein (Torraco et al., 2018) inducing a large decrease of *ISCA1* protein level in fibroblasts. Concerning the other known mutation in *ISCA1*, p.(Gln87Lys), no functional analysis was performed to understand the mechanism of the pathogenicity of this mutation. In all the described patients, dysfunction of *ISCA1* also causes abnormal respiratory chain and lipoylated protein functionalities. In fibroblasts and/or myoblasts of our studied patient, activities of complexes I and II were affected probably by defect of maturation of their Fe-S cluster containing subunits such as SDHB for complex II. BN-PAGE analysis showed an altered assembly of these two complexes but also of complex IV. Activities of PDH and α -KGDH complexes were moderately decreased in fibroblasts or myoblasts secondary to limited lipoylation defect. The effect was clearly less severe than for the Italian patient (Torraco et al., 2018). Surprisingly, deleterious biochemical consequences of the mutation were not more pronounced in myoblasts than in fibroblasts. As in several MMDS (Ajit Bolar et al., 2013; Lebigot et al., 2017; Ahting et al., 2015; Nishioka et al., 2018), complex IV is also affected in MMDS type 5 either with decrease of total complex IV assembly (present report) or decrease of a complex IV subunit with unknown mechanism (Torraco et al., 2018). Importantly, all the results show that the *ISCA1* Tyr101Cys mutant functionally impaired mitochondrial [4Fe-4S] proteins assembly and was causative of the observed clinical features. Despite dysfunctions of many RC complexes, we observed that the mitochondrial network did not show fragmented morphology in fibroblasts. The repartition of mitochondria is homogeneous in cytoplasm compared to results obtained in fibroblasts of one *ISCA2* patient (Alaimo et al., 2018). Two studies suggested that complete *ISCA1* deficiency was unsustainable in mammals (Beilschmidt et al., 2017; Yang et al., 2019) and would be lethal at the embryo state in rats (Yang et al., 2019). Even if *ISCA1* was severely decreased in the patient fibroblasts, we hypothesized that residual *ISCA1* functionality must be present in tissues others than fibroblasts for the French *ISCA1* patient who presented with moderate clinical phenotype.

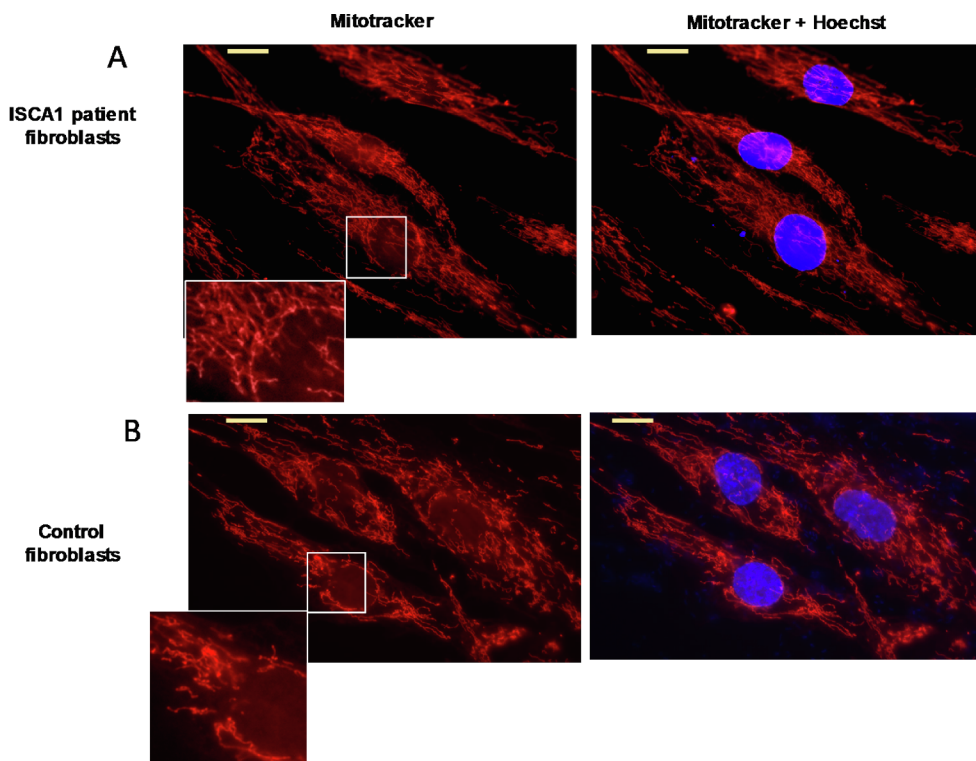


Fig. 8. Mitochondrial network in *ISCA1* patient fibroblasts. Mitochondria of patient fibroblasts were labelled with the Mitotracker probe (A) and compared to control fibroblasts (B). Hoechst was used to counterstain the nuclei as indicated in the figure (right panel). The inset shows a magnification of the selected mitochondrial subcellular region (white square). Scale bar represents 10 μ m.

ISCA1 is one of the proteins involved in the late step of maturation of ISC containing protein but its functionality inside this machinery is not clearly known as yet. Since 2004, mitochondrial localization of *ISCA1* was proven and its role in Fe-S cluster biogenesis was proposed (C  zar-Castellano et al., 2004). Further studies in HeLa cells suggested that *ISCA1* collaborates with *ISCA2* and *IBA57* in the late step of the maturation of mitochondrial Fe-S proteins (Sheftel et al., 2012). Recently, *in vitro* studies demonstrated that the biogenesis of [4Fe-4S] cluster from two [2Fe-2S] clusters required *ISCA1* and *ISCA2* proteins (Brancaccio et al., 2014; Brancaccio et al., 2017). Other analyses suggested that homodimeric *ISCA1* could be sufficient to form a [4Fe-4S] cluster from two [2Fe-2S] clusters (Beilschmidt et al., 2017). Finally, *IBA57* and *ISCA2* may also collaborate with *ISCA1* for [4Fe-4S] cluster biogenesis (Gourdoupis et al., 2018). Interestingly, a study revealed that *ISCA2* protein was decreased in fibroblasts of an *ISCA1* patient (Torraco et al., 2018) while *ISCA1* protein level was not decreased in fibroblasts of an *ISCA2* patient (this study). These results suggest that *ISCA2* required *ISCA1* to be stabilized but *ISCA1* is not destabilized by low level of *ISCA2* in the same tissue. *ISCA1* and *ISCA2* are able to interact with each other but are not redundant in their functions in ISC machinery. With recent *in vitro* studies and multiple descriptions of MMDS type 5, it appears that *ISCA1* protein is an essential protein for maturation of ISC-containing protein. *ISCA1* deficiency leads to biochemical and clinical consequences similar to those reported in *IBA57* or *ISCA2* deficiency, all involved in the late steps of mitochondrial [4Fe-4S] cluster biogenesis.

In conclusion, we report a patient with spastic diplegia and severe language delay who carries a novel pathogenic variant in *ISCA1*. This Tyr101Cys variant clearly destabilizes the Fe-S cluster of the *ISCA1* protein and reduces stability and functionality of this latter. Mitochondrial [4Fe-4S]-containing proteins such as subunits of RC complexes or proteins involved in lipoic acid synthesis are therefore affected by *ISCA1* dysfunction, leading to MMDS type 5.

Acknowledgements

We thank the AMMI association (Association contre les Maladies Mitochondriales) for its financial contribution to this work. We thank

Allison CARDOSO and Yannick SANDRE for their technical help. We are grateful for the excellent expertise from Dr Abdel SLAMA during this work.

References

- Braymer, J.J., Lill, R., 2017. Iron-sulfur cluster biogenesis and trafficking in mitochondria. *J. Biol. Chem.* 292 (31), 12754–12763.
- Beilschmidt, L.K., Puccio, H.M., 2014. Mammalian Fe-S cluster biogenesis and its implication in disease. *Biochimie* 100, 48–60.
- Brancaccio, D., Gallo, A., Mikolajczyk, M., Zovo, K., Palumaa, P., Novellino, E., et al., 2014. Formation of [4Fe-4S] clusters in the mitochondrial iron-sulfur cluster assembly machinery. *J. Am. Chem. Soc.* 136 (46), 16240–16250.
- Brancaccio, D., Gallo, A., Piccioli, M., Novellino, E., Ciofi-Baffoni, S., Banci, L., 2017. [4Fe-4S] cluster assembly in mitochondria and its impairment by copper. *J. Am. Chem. Soc.* 139 (2), 719–730.
- Cameron, J.M., Janer, A., Levandovskiy, V., Mackay, N., Rouault, T.A., Tong, W.-H., et al., 2011. Mutations in iron-sulfur cluster scaffold genes *NFU1* and *BOLA3* cause a fatal deficiency of multiple respiratory chain and 2-oxoacid dehydrogenase enzymes. *Am. J. Hum. Genet.* 89 (4), 486–495.
- Melber, A., Na, U., Vashisht, A., Weiler, B.D., Lill, R., Wohlschlegel, J.A., et al., 2016. Role of *Nfu1* and *Bol3* in iron-sulfur cluster transfer to mitochondrial clients. *Elife* 5 (August), e15991.
- Sheftel, A.D., Wilbrecht, C., Stehling, O., Niggemeyer, B., Els  sser, H.-P., M  hlenhoff, U., et al., 2012. The human mitochondrial *ISCA1*, *ISCA2*, and *IBA57* proteins are required for [4Fe-4S] protein maturation. *Mol. Biol. Cell* 23 (7), 1157–1166.
- Ajit Bolar, N., Vanlander, A.V., Wilbrecht, C., Van der Aa, N., Smet, J., De Paepe, B., et al., 2013. Mutation of the iron-sulfur cluster assembly gene *IBA57* causes severe myopathy and encephalopathy. *Hum. Mol. Genet.* 22 (13), 2590–2602.
- Gourdoupis, S., Nasta, V., Calderone, V., Ciofi-Baffoni, S., Banci, L., 2018. *IBA57* recruits *ISCA2* to form a [2Fe-2S] cluster-mediated complex. *J. Am. Chem. Soc.* 140 (43), 14401–14412.
- Shukla, A., Hebbar, M., Srivastava, A., Kadavigere, R., Upadhyay, P., Kanthi, A., et al., 2017. Homozygous p. (Glu87Lys) variant in *ISCA1* is associated with a multiple mitochondrial dysfunctions syndrome. *J. Hum. Genet.* 62 (7), 723–727.
- Shukla, A., Kaur, P., Girisha, K., 2018. Report of the third family with multiple mitochondrial dysfunctions syndrome 5 caused by the founder variant p.(Glu87Lys) in *ISCA1*. *J. Pediatr. Genet.* 07 (03), 130–133.
- Torraco, A., Stehling, O., St  mpfig, C., R  sser, R., De Rasmus, D., Fiermonte, G., et al., 2018. *ISCA1* mutation in a patient with infantile-onset leukodystrophy causes defects in mitochondrial [4Fe-4S] proteins. *Hum. Mol. Genet.* 27 (15), 2739–2754.
- Imbard, A., Boutron, A., Vequaud, C., Zater, M., De Lonlay, P., Ogier de Baulny, H., et al., 2011. Molecular characterization of 82 patients with pyruvate dehydrogenase complex deficiency. Structural implications of novel amino acid substitutions in E1 protein. *Mol. Genet. Metab.* 104 (4), 507–516.
- Rustin, P., Chretien, D., Bourgeron, T., G  rard, B., R  tig, A., Saudubray, J.M., et al., 1994.

- Biochemical and molecular investigations in respiratory chain deficiencies. Clin. Chim. Acta 228 (1), 35–51.
- Chretien, D., Bénit, P., Chol, M., Lebon, S., Rötig, A., Munnich, A., et al., 2003. Assay of mitochondrial respiratory chain complex I in human lymphocytes and cultured skin fibroblasts. Biochem. Biophys. Res. Commun. 301 (1), 222–224.
- Hescot, S., Slama, A., Lombès, A., Paci, A., Remy, H., Leboulleux, S., et al., 2013. Mitotane alters mitochondrial respiratory chain activity by inducing cytochrome c oxidase defect in human adrenocortical cells. Endocr. Relat. Cancer 20 (3), 371–381.
- Bouali, N., Francou, B., Bouligand, J., Imanci, D., Dimassi, S., Tosca, L., et al., 2017. New MCM8 mutation associated with premature ovarian insufficiency and chromosomal instability in a highly consanguineous Tunisian family. Fertil. Steril. 108 (4), 694–702.
- Bradford, M., 1976. A rapid and sensitive method for the quantitation of microgram quantities of protein utilizing the principle of protein-dye binding. Anal. Biochem. 72 (1–2), 248–254.
- Fish, W.W. [27] Rapid colorimetric micromethod for the quantitation of complexed iron in biological samples. Methods in enzymology. 1988. pp. 357–364.
- Beilshmidt, L.K., Ollagnier de Choudens, S., Fournier, M., Sanakis, I., Hograindleur, M.-A., Clémancey, M., et al., 2017. ISCA1 is essential for mitochondrial Fe4S4 biogenesis in vivo. Nat. Commun. 8 (May), 15124.
- Lebigot, E., Gaignard, P., Dorboz, I., Slama, A., Rio, M., de Lonlay, P., et al., 2017. Impact of mutations within the [Fe-S] cluster or the lipoic acid biosynthesis pathways on mitochondrial protein expression profiles in fibroblasts from patients. Mol. Genet. Metab. 122 (3), 85–94.
- Landgraf, B.J., McCarthy, E.L., Booker, S.J., 2016. Radical S-adenosylmethionine enzymes in human health and disease. Annu. Rev. Biochem. 4 (85), 485–514.
- Wai, T., Langer, T., 2016. Mitochondrial dynamics and metabolic regulation. Trends Endocrinol. Metab. 27 (2), 105–117.
- Lossos, A., Stümpfig, C., Stevanin, G., Gaussen, M., Zimmerman, B.-E., Mundwiler, E., et al., 2015. Fe/S protein assembly gene IBA57 mutation causes hereditary spastic paraplegia. Neurology. 84 (7), 659–667.
- Debray, F.-G., Stümpfig, C., Vanlander, A.V., Dideberg, V., Josse, C., Caberg, J.-H., et al., 2015. Mutation of the iron-sulfur cluster assembly gene IBA57 causes fatal infantile leukodystrophy. J. Inherit. Metab. Dis. 38 (6), 1147–1153.
- Al-Hassnan, Z.N., Al-Dosary, M., Alfadhel, M., Faqeih, E.A., Alsagob, M., Kenana, R., et al., 2015. ISCA2 mutation causes infantile neurodegenerative mitochondrial disorder. J. Med. Genet. 52 (3), 186–194.
- de Souza, P.V.S., Bortholin, T., Burlin, S., Naylor, F.G.M., Pinto, W.B.V. de R., Oliveira, A.S.B., 2018 Mar. NFU1-related disorders as key differential diagnosis of cavitating leukoencephalopathy. J. Pediatr. Genet. 7 (1), 40–42.
- Ishiyama, A., Sakai, C., Matsushima, Y., Noguchi, S., Mitsuhashi, S., Endo, Y., et al., 2017. IBA57 mutations abrogate iron-sulfur cluster assembly leading to cavitating leukoencephalopathy. Neurol. Genet. 3 (5), e184.
- Torraco, A., Ardisson, A., Invernizzi, F., Rizza, T., Fiermonte, G., Niceta, M., et al., 2017. Novel mutations in IBA57 are associated with leukodystrophy and variable clinical phenotypes. J. Neurol. 264 (1), 102–111.
- Hamanaka, K., Miyatake, S., Zerem, A., Lev, D., Blumkin, L., Yokochi, K., et al., 2018. Expanding the phenotype of IBA57 mutations: related leukodystrophy can remain asymptomatic. J. Hum. Genet. 63, 1223–1229.
- Liu, M., Zhang, J., Zhang, Z., Zhou, L., Jiang, Y., Wang, J., et al., 2018. Phenotypic spectrum of mutations in IBA57, a candidate gene for cavitating leukoencephalopathy. Clin. Genet. 93 (2), 235–241.
- Alfadhel, M., Nashabat, M., Alrifai, M.T., Alshaalan, H., Al Mutairi, F., Al-Shahrani, S.A., et al., 2018. Further delineation of the phenotypic spectrum of ISCA2 defect: a report of ten new cases. Eur J Paediatr Neurol. 22 (1), 46–55.
- Alaimo, J.T., Besse, A., Alston, C.L., Pang, K., Appadurai, V., Samanta, M., et al., 2018. Loss-of-function mutations in ISCA2 disrupt 4Fe-4S cluster machinery and cause a fatal leukodystrophy with hyperglycemia and mtDNA depletion. Hum. Mutat. 39 (4), 537–549.
- Toldo, I., Nosadini, M., Boscardin, C., Talenti, G., Manara, R., Lamantea, E., et al., 2018. Neonatal mitochondrial leukoencephalopathy with brain and spinal involvement and high lactate: expanding the phenotype of ISCA2 gene mutations. Metab. Brain Dis. 33, 805–812.
- Ahting, U., Rolinski, B., Haack, T.B., Mayr, J.A., Alhaddad, B., Prokisch, H., et al., 2015. FeS cluster biogenesis defect in a patient with mutations in ISCA2. J. Inherit. Metab. Dis. 38 (Suppl1), S218.
- Nishioka, M., Inaba, Y., Motobayashi, M., Hara, Y., Numata, R., Amano, Y., et al., 2018. An infant case of diffuse cerebrosplinal lesions and cardiomyopathy caused by a BOLA3 mutation. Brain Dev. 40 (6), 484–488.
- Yang, X., Lu, D., Zhang, X., Chen, W., Gao, S., Dong, W., et al., 2019. Knockout of ISCA 1 causes early embryonic death in rats. Anim. Model Exp. Med. 2 (1), 18–24.
- Cózar-Castellano, I., del Valle, Machargo M, Trujillo, E., Arteaga, M.F., González, T., Martín-Vasallo, P., et al., 2004. hIsC: a protein implicated in the biogenesis of iron-sulfur clusters. Biochim. Biophys. Acta 1700 (2), 179–188.